AMERICAN SOCIETY of
GENE & CELL
THERAPY

Universal RNAi Triggers for the Specific Inhibition of Mutant Huntingtin, Atrophin-1, Ataxin-3, and Ataxin-7 Expression

Anna Kotowska-Zimmer,[1] Yuliya Ostrovska,[1] and Marta Olejniczak[1,2]

[1]Department of Genome Engineering, Institute of Bioorganic Chemistry, Polish Academy of Sciences, Noskowskiego 12/14, 61-704 Poznan, Poland; [2]Dystrogen Gene Therapies, 1415 W 37th Street, Chicago, IL, USA

The expansion of CAG repeats within the coding region of associated genes is responsible for nine inherited neurodegenerative disorders including Huntington's disease (HD), spinocerebellar ataxias (SCAs), and dentatorubral-pallidoluysian atrophy (DRPLA). Despite years of research aimed at developing an effective method of treatment, these diseases remain incurable and only their symptoms are controlled. The purpose of this study was to develop effective and allele-selective genetic tools for silencing the expression of mutated genes containing expanded CAG repeats. Here we show that repeat-targeting short hairpin RNAs preferentially reduce the levels of mutant huntingtin, atrophin-1, ataxin-3, and ataxin-7 proteins in patient-derived fibroblasts and may serve as universal allele-selective reagents for polyglutamine (polyQ) diseases.

INTRODUCTION

Polyglutamine (polyQ) diseases are a group of inherited autosomal dominant neurological disorders caused by the expansion of unstable CAG repeats in translated regions of the respective genes. There are 9 known polyQ diseases, including Huntington's disease (HD), six spinocerebellar ataxias (SCA) types 1, 2, 3, 6, 7, 17; dentatorubral-pallidoluysian atrophy (DRPLA); and spinal and bulbar muscular atrophy (SBMA). The common pathogenic factor in this group of disorders is toxic protein with a polyQ domain that forms intracellular aggregates and causes neuronal degeneration and death. The pathology related to polyQ diseases develops in the specific brain areas characteristic of each disorder, e.g., striatum and cerebral cortex in HD, or cerebellum, basal ganglia, brainstem, and spinal cord in SCA3.[1–4]

Although no causal therapy is currently available and only symptomatic treatment is offered to patients, many therapeutic approaches are being tested to reverse or slow the progression of the disease.[5,6] Because the pathogenesis of polyQ diseases is associated with the presence of toxic proteins, the most direct therapeutic strategies involve silencing of the specific gene expression with the use of antisense oligonucleotides (ASO) and RNA interference (RNAi), preventing mutant protein aggregation, inhibiting the cleavage of polyQ proteins and inducing mutant protein degradation.[6–9] Other promising results were obtained by targeting downstream cellular effects,

such as reduction of mitochondrial dysfunction and oxidative stress or decrease of inflammation.[10–13] Recently successful editing of HTT and ATXN3 genes with the use of the CRISPR-Cas9 system was demonstrated.[14–18] However, safety issues related to the permanent modification of the genome and off-target effects need to be resolved before clinical application of therapy.

In recent years, groundbreaking research has been conducted on HD therapy. Of particular importance are three publications reporting three different technologies.[19–21] The first publication summarizes the results of a Phase 1/2a clinical trial with repeated injections of ASO in early manifest HD patients.[19] In the second study, the authors demonstrate efficient allele-selective transcriptional repression of the mutant HTT with the use of zinc finger protein transcription factors (ZFP-TF) in cell cultures and mouse models.[20] Finally, in the last study, a single injection of fully modified small interfering RNA (siRNA) (divalent siRNA, di-siRNA) into the cerebrospinal fluid resulted in potent, sustained gene silencing in the central nervous system (CNS) of mice and nonhuman primates.[21]

Because the function of the wild-type polyQ proteins and their roles through patient lifetime is incompletely understood, the safest therapeutic strategy is to target mutant variants, leaving the normal proteins intact. For polyQ disease genes, the regions differentiating the alleles that can be selectively targeted are single-nucleotide polymorphisms (SNPs) linked to the repeat expansions and the repeat region itself. The first strategy has some limitations because SNPs that are targets for ASOs are present only in a selected group of patients.[22–24] However, a Phase 1b/2a clinical trial of allele-selective ASOs targeting two SNPs (rs362307 and rs362331) in early manifest HD patients is ongoing (https://www.clinicaltrials.gov/, ClinicalTrials.gov: NCT03225833 and NCT03225846). A more universal strategy, applicable for all patients, is based on the difference between

the repeat tract length in the normal and mutant alleles. By using different types of CAG-targeting oligonucleotides in different polyQ models, the David Corey group showed the potency of this strategy in allele-selective silencing of mutant proteins.[25–29] In our previous study, we demonstrated successful silencing of mutant huntingtin expression using a CAG repeat-targeting strategy and RNAi tools.[30] The introduction of selective modifications into siRNA sequences creates mismatches with mRNA targets and activation of microRNA (miRNA)-like translation inhibition mechanisms.[27,30,31] Preferential silencing of mutant alleles is achieved by binding of more silencing complexes to long CAG repeat tracts.

The activity and allele selectivity of selected chemically modified CAG-targeting siRNA oligonucleotides were also confirmed in SCA3, SCA7, and DRPLA models.[26,32–34] However, in preclinical and clinical applications, RNAi triggers are generally delivered as viral vectors to provide long-term expression and broad distribution of reagents in affected brain regions. Vector-based short hairpin RNAs (shRNAs) and artificial miRNAs expressed in cells from Pol III (typically H1 promoter of RNase P or U6 small nuclear RNA [snRNA] promoter) or Pol II promoters mimic pre- and pri-miRNA precursors, respectively. They are processed in cells by miRNA biogenesis machinery to form mature siRNA. Transcribed shRNAs are transported from nucleus to the cytoplasm by the Exportin-5/Ran guanosine triphosphate (GTP) complex and undergo single step processing by endoribonuclease Dicer. Processing is, however, imprecise and depends on the sequence and structure of a molecule and generates a heterogeneous pool of siRNAs.[35] Therefore, the activity of siRNAs, especially those containing selective sequence modifications, is not always reflected in corresponding vector-based RNAi triggers.[36,37]

In the current study, we analyzed the efficacy and allele selectivity of CAG repeat-targeting reagents expressed in cells as shRNAs. We demonstrated that shRNAs efficiently silence the expression of mutant *HTT*, *ATN1*, *ATXN3*, and *ATXN7* genes in patient-derived fibroblasts. We confirmed that shRNAs are processed in cells by Dicer into a pool of siRNA with a predominance of the desired guide strand variant, which did not induce a significant off-target effect in a fibroblast model of the disease.

RESULTS
Preferential Inhibition of Mutant Huntingtin Expression by CAG-Targeting shRNAs

The CAG repeat-targeting strategy uses reagents comprising complementary CUG repeats. Therefore, in the first step, we designed shRNAs with a stem consisting of pure CUG/CUG and CAG/CUG repeats (Figure S1A). The hairpin, comprising CUG repeats, is processed by Dicer with low efficiency, likely due to the instability of the stem structure containing periodic U:U mismatches (Figure S1B). This results in low activity toward CAG-containing transcripts. More typical CAG/CUG shRNA with perfectly paired stem is processed into a pool of siRNA with high efficiency; however, its silencing activity is non-allele selective (Figure S1C).

In our previous study, we demonstrated that siRNAs containing specific interruptions in the CUG sequence (U > A and U > G type) are selective toward mutant huntingtin in cellular models of HD.[30] siRNA efficacy and selectivity were dependent on the type of modification and their number and position within the siRNA guide strand. The most active A2 siRNA was designed to form two variants of shRNAs (driven by the H1 promoter), namely, A2R and A2R1, comprising the hsa-miR-23 loop and CAG/CUG stem with a single U > A modification. We confirmed that shRNAs were processed in cells by Dicer into a pool of 19–24 nt siRNA and efficiently reduced mutant huntingtin levels by 90%, leaving the normal huntingtin intact.[30]

To examine the allele selectivity of other siRNA variants expressed from genetic vectors in this study, we designed two other shRNAs containing single (shG2) or two (shG4) U > G substitutions at specific positions of the CUG repeat strand, resulting in the formation of the G-A mismatches with the target transcript.

To analyze the products of shRNAs processing by Dicer, we transfected HEK 293T cells with plasmids encoding shRNAs and performed NGS analysis of small RNA. As expected, the analyzed reagents exhibit similar strand biases, with a considerable predominance of the guide siRNA strands originating from the 3′ arm, reaching more than 99% for shA2R (Figure 1A), shG2, and shG4 and 96% for shA2R1 (Figure S2). Corresponding siRNAs derived from the shA2R and shG2 differed mainly in length of the U-tail at their 3′ ends, whereas 90% of molecules contain an A or G substitution at position 8 from the 5′ end (5′-CTGCTGCNGCTGCTGCTGCTT-3′). siRNAs derived from shA2R1 were represented by two main variants shifted at the 5′ end, which resulted in A substitution at position 8 (69%) and position 9 (25%) from the 5′ end. In the case of shG4, the main variant represented by 95% of siRNAs contains G substitution at positions 8 and 14 from the 5′ end (Figure S2).

To evaluate the potency of the shRNA constructs *in vitro*, we cotransfected them into HEK 293T cells together with luciferase (Luc) reporters bearing either the human *HTT* exon 1 encompassing 85 CAG repeats (mutant, 85CAG_Luc) or 16 CAG repeats (normal, 16CAG_Luc). We obtained significant repression of the luciferase expression after the transfection of 85CAG_Luc with all of the shRNA constructs; the knockdown effect was stronger than 60% for all shRNAs with shA2R being the most efficient and inducing ±75% silencing of mutant HTT (Figures 1B and 1C). An analysis of the half maximal inhibitory concentration (IC_{50}) values indicates that shG2, shA2R, and shA2R1 are more potent than shG4 and knock down the tested 85CAG_Luc reporter by 50% in concentration of 10 ng, 13.5 ng, and 16.3 ng, respectively (Figure 1C). The 16CAG_Luc reporters were not knocked down by 50% even in the highest concentration of shRNAs tested (500 ng). The highest allele selectivity measured as the ratio of the IC_{50} values ($IC_{5016CAG\_Luc}/IC_{5085CAG\_Luc}$) was achieved when shG2 (>50) and shA2R (>37) were used (Figure 1C).
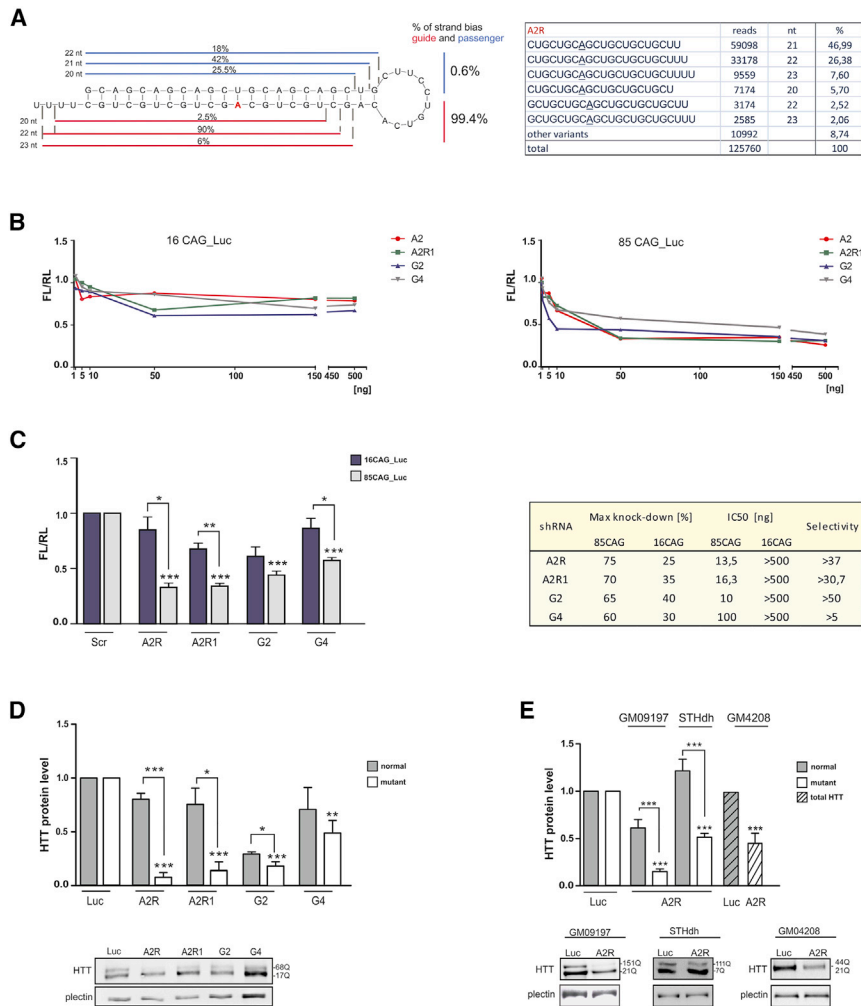
Figure 1. Cellular Processing of shA2R and Silencing Activity of CAG-Targeting shRNAs in HD Models

(A) Next-generation sequencing analysis of the shA2R processing pattern in HEK 293T cells. The guide strand is indicated in red, and the passenger strand is indicated in blue. Cleavage sites are presented on both strands corresponding to the length of released siRNA variants (content and length are noted on the left site). The table presents the results of total quantity reads, length, and percentage content of the sequence composition of released strands after NGS analysis. (B) Knockdown of Luciferase (Luc) reporters containing exon 1 of the *HTT* gene with 16 CAG repeats (16CAG_Luc) or 85 CAG repeats by shA2R, A2R1, G2, and G4. The *HTT* gene fragment was fused to the firefly luciferase (FL) gene and renilla luciferase (RL) was used as an internal control. HEK 293T cells were co-transfected with 50 ng of Luc reporters and 1, 5, 10, 50, 150, or 500 ng of shRNA constructs. FL and RL were measured 2 days posttransfection and FL was normalized to RL expression. A scrambled construct (shScr) served as a negative control and relative repression of luciferase expression following the transfection of the shScr reporter was set at 1. (C) The graph represents the results of Luc reporters' knockdown by shRNA constructs used in the concentration of 50 ng (1×1 ratio of Luc reporter and shRNA). Maximal knockdown by four shRNAs (%), the half maximal inhibitory concentration (IC_{50}), and allele selectivity is demonstrated in the table. The value of IC_{50} indicates a concentration (ng) of a shRNA construct that is required for 50% Luc reporter knockdown. The selectivity was calculated as the IC_{50} ratio of 16CAG_Luc/85CAG_Luc. (D) Western blot analysis of HTT levels in HD patient-derived fibroblasts (cell line GM04281, 17/68Q) at 7 days posttransduction with LV in MOI of 10, containing shA2R, shA2R1, shG2, and shG4 expression cassettes. Signal intensities of the protein level were normalized to plectin protein levels and compared using a one-sample t test. (E) Western blot analysis of HTT levels in different cell lines: human HD fibroblasts (GM09197 – 21/151Q, GM04208 – 21/41Q) and HD mouse striatal

precursor cell line STHdh (7/111Q). Because the difference between normal and mutant protein in the cell line GM04208 (21/41Q) is low and separation of these two variants is very difficult, we measured total huntingtin level as described in the graph. The shLuc construct was used as a control reference in both graphs. The graph bars represent the mean value of protein levels ± SEM. The p values are indicated by asterisks (*p < 0.05, **p < 0.01, ***p < 0.001). All experiments were repeated at least three times.

Next, we analyzed the silencing efficiency of the shRNAs in a cellular model of HD. shRNAs were introduced into HD patient-derived fibroblasts (GM04281; 68 CAG repeats/mutant allele, 17 CAG repeats/wild-type allele) by lentiviral transduction, and protein was isolated at 7 days posttransduction. Analysis of huntingtin levels by western blotting demonstrated ∼70% and 50% reduction of mutant protein levels by shG2 and shG4, respectively (Figure 1D). However, in the case of shG2, the normal huntingtin was also significantly reduced by ∼60%. Interestingly, the only difference between allele-selective shA2R and nonselective shG2 is the type of substitution within the CUG guide strand (U > A versus U > G). As confirmed by NGS, these molecules are processed into similar siRNA variants with nucleotide substitution at position 8. The transcript level measured by quantitative real-time PCR did not decrease after lentiviral (LV) shRNA transduction (Figure S3), and this finding may indicate a predominance

of the translation inhibition mechanism of action suggested in other studies using miRNA-like siRNA.

Next, we examined the inhibition of HTT and allele selectivity in other HD cellular models with different numbers of CAG tracts (fibroblasts GM04208 with 21/44 CAG, GM09197 with 21/151 CAG, and mouse neuronal precursors STHdh with 7/111 Q) (Figure 1E). In all cases, shA2R preferentially silenced the expression of the mutant *HTT* gene; however, the transduction efficiency of the STHdh cell line was lower than that for human fibroblasts, which is reflected in the total silencing efficiency.

CAG-Targeting shRNAs Silence the Expression of *ATN1*, *ATXN3*, and *ATXN7* Genes

To determine whether CAG-targeting shRNAs could be considered universal therapeutics for polyQ diseases, we transduced DRPLA
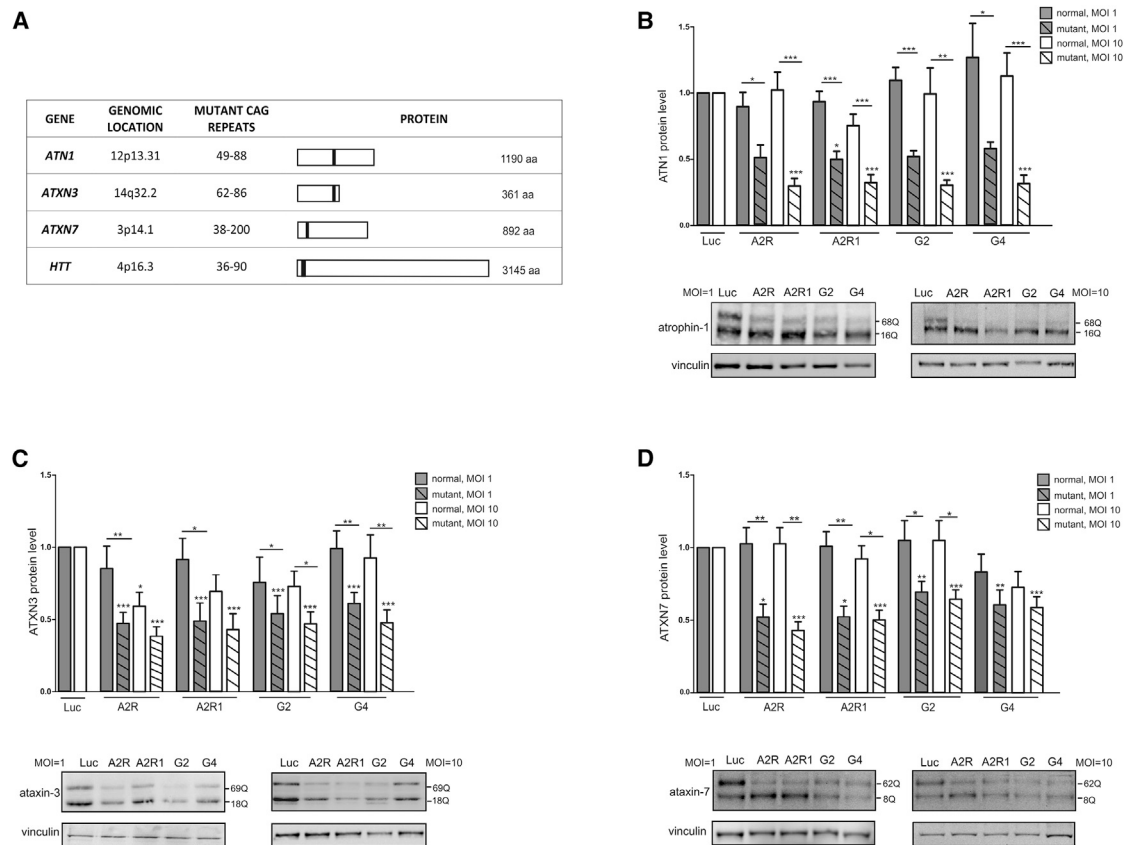
Figure 2. Analysis of Efficacy and Allele Selectivity of CAG-Targeting shRNAs in Cellular Models of DRPLA, SCA3, and SCA7

(A) Characterization of polyQ models used in this study. (B–D) Western blot analysis of atrophin-1 levels in DRPLA patient-derived fibroblasts (16/68Q) (B), ataxin-3 levels in SCA3 patient-derived fibroblasts (18/69Q) (C), and ataxin-7 levels in SCA7 patient-derived fibroblasts (8/62Q) (D). Protein was isolated at 7 days posttransduction with two concentrations of LV (MOI of 1 and 10) containing shA2R, shA2R1, shG2, and shG4 expression cassettes. The shLuc construct (Luc) was used as a negative control. Signal intensities of the protein level were normalized to vinculin protein level and compared using a one-sample t test. The graph bars represent the mean value of protein levels ± SEM. The p values are indicated by asterisks (*p < 0.05, **p < 0.01, ***p < 0.001). All experiments were repeated at least three times.

(16/68 CAG), SCA3 (18/69 CAG), and SCA7 (8/62 CAG) patient-derived fibroblasts with two concentrations of LV (multiplicity of infection [MOI] of 1 and 10) expressing shA2R, shA2R1, shG2, and shG4. These models differ in terms of CAG tract localization within specific genes, chromosomal environment and localization of causative genes, and the threshold of pathogenic repeat number (Figure 2A).

DRPLA is caused by the expansion of the CAG tract to ≥ 49 repeats in the *ATN1* gene localized at 12p13.31. In patient-derived fibroblasts containing 16/68 CAG repeats, all tested shRNAs demonstrated allele-selective silencing of mutant atrophin-1 by ∼50% in lower concentration of LVs and ∼70% in MOI of 10 (Figure 2B). Stronger discrimination between alleles was observed in higher concentration of LV particles.

SCA3, also known as Machado-Joseph disease (MJD), is caused by the expansion of the CAG tract to more than 62 repeats within exon 10 of the *ATXN3* gene localized at chromosome 14q32.1. In contrast to the HD model, shRNAs of A- and G-type showed a similar pattern of ac-

tivity and preferentially silenced the expression of the mutant allele to ∼50% of the control level (Figure 2C). However, silencing efficacy and allele selectivity was lower than for the HD and DRPLA models, and the most efficient shA2R reduced mutant and normal ataxin-3 by ∼60% and ∼40%, respectively. Generally, the silencing efficiency increased slightly with a higher dose of LV particles and also resulted also in lower allele selectivity.

Another example of polyQ diseases is SCA7 caused by the expansion of >38 CAG repeats at the *ATXN7* gene localized on chromosome 3p14.1. Similar to HD, the abnormal polyQ tract is localized in the N-terminal part of the protein. In a fibroblast model containing 8 and 62 CAG repeats, shA2R demonstrated the greatest efficacy and allele discrimination, with normal ataxin-7 unaffected and mutant silenced nearly by 60% (Figure 2D). In contrast to DRPLA and SCA3 models, and similar to HD model, shG4 decreased the level of normal and mutant ATXN7 by approximately 20% and 40%, respectively. However, overall ATXN-7 target silencing by analyzed shRNAs was the lowest among all polyQ models.
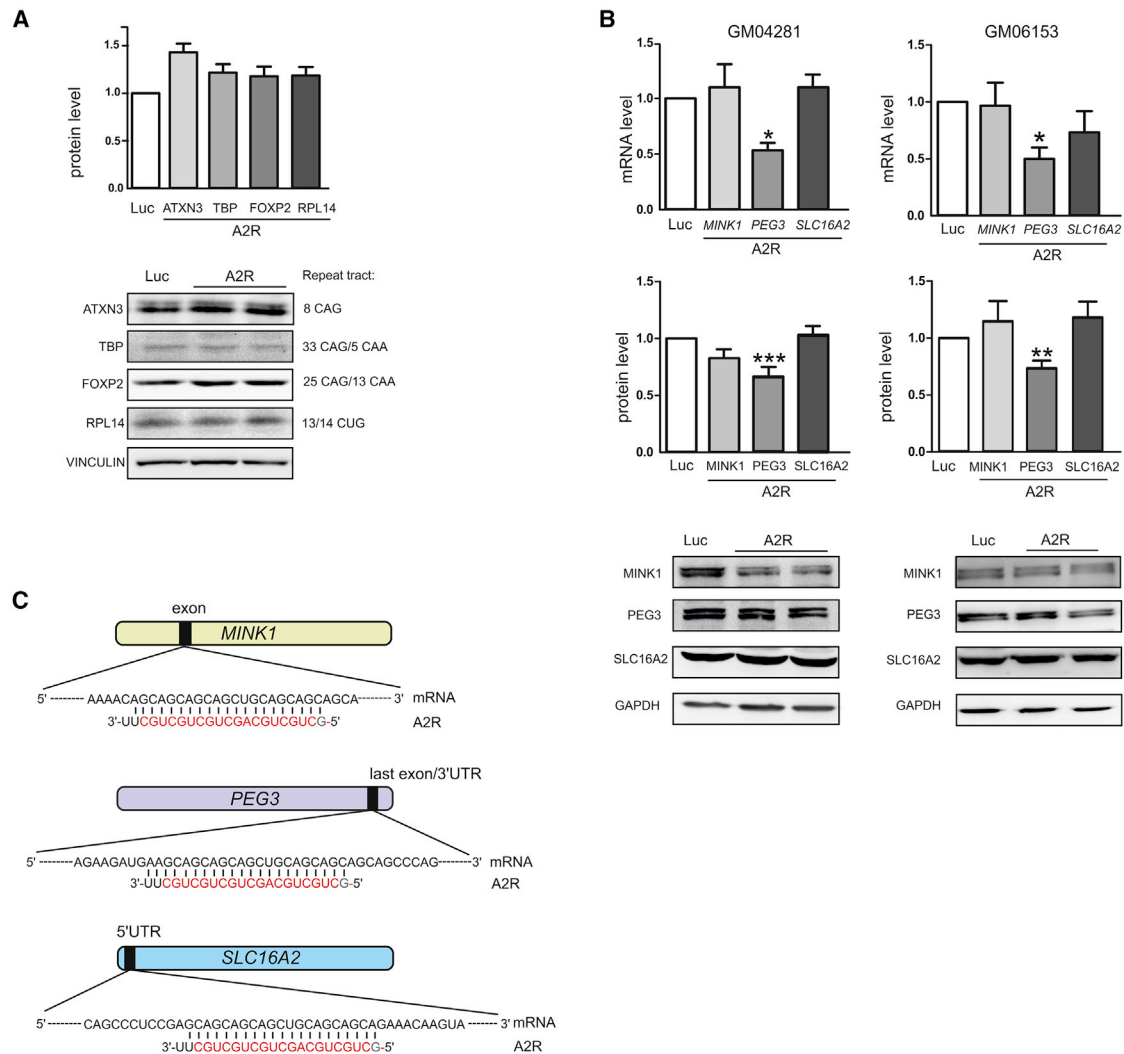
Figure 3. Evaluation of Off-Target Effects Induced by the shA2R in Human Fibroblasts

(A) Western blot analysis of selected proteins containing pure or interrupted CAG repeats in respective genes. Protein level was analyzed after transduction of HD fibroblasts (GM04281) with LV in MOI of 10 containing shA2R expression cassette. The signal intensities of the protein level were normalized to vinculin level and compared using a one-sample t test. (B) Analysis of mRNA transcript level (quantitative real-time PCR) and protein level (western blotting) of predicted off-target genes: *MINK1*, *PEG3*, and *SLC16A2*. Analysis was performed in HD (GM04281) and SCA3 (GM06153) patient-derived fibroblasts treated with LV in MOI of 10 containing shA2R expression cassette. GAPDH was used as a reference protein. (C) The localization of the target sequence within the MINK1, PEG3, and SLC16A2 transcripts with full complementarity to the shA2R reagent. The shLuc (Luc) construct was used as a control reference. The graph bars represent the mean value of protein or transcript levels ± SEM. The p values are indicated by asterisks (*p < 0.05, **p < 0.01, ***p < 0.001). All experiments were repeated at least three times.

Although in each polyQ model, the shRNAs demonstrated different patterns of silencing, shA2R seems to be a candidate universal therapeutic tool for these diseases.

CAG-Targeting shRNA Does Not Generate Significant Off-Target Effects

An important challenge for therapeutic molecules that target CAG repeats is the existence of other genes that contain similar repetitive regions.[38] Previously, we demonstrated the gene selectivity of CAG-targeting siRNAs by analyzing the cellular levels of other proteins encoded by genes containing pure or interrupted CAG repeats (ATXN3; TATA-box binding protein, TBP, and FOXP2) and CTG repeats (EIF2AK3, RPL14, and LRP8).[30] The Corey group[27] observed no inhibition of TBP, androgen receptor, AAK-1, POU3F2, or FOXP2 at high concentrations of CAG-targeting oligonucleotides. In this study, we confirmed these results by analyzing TBP (33 CAG with 5 CAA interruptions), FOXP2 (25 CAG with 13 CAA), RPL14 (13/14 CUG), and ATXN3 (8 CAG) protein levels in HD fibroblasts treated with shA2R. None of these proteins was inhibited (Figure 3A). This finding

supports the translation inhibition mechanism by miRNA-like siRNA in which only longer, uninterrupted CAG tracts are efficiently blocked by RISC-CUG.

We also performed bioinformatic analysis (BLAST NCBI and Ensembl blast) of mRNA targets that are fully complementary to the shA2R guide strand because this type of interaction may induce AGO2-mediated mRNA cleavage and unintended reduction of some transcript levels (Table S1). Guide strands released from shA2R (with U > A substitution at position 8 or 9) have 5 mRNA targets with full complementarity of 21 nt, 7 targets with 20 nt complementarity, 1 target with 19 nt, and 7 targets with 18 nt complementarity. Misshapen-like kinase 1 (MINK1), paternally expressed gene 3 (PEG3) and solute carrier family 16 member 2 (SLC16A2) transcripts were expressed in fibroblasts, and we analyzed their levels by qPCR after shA2R treatment. Of these three transcripts, only the PEG3 level was decreased by ∼50% in HD and SCA3 fibroblasts (Figure 3B). A protein level analysis confirmed that only PEG3 is downregulated by ∼30% in human fibroblasts (Figure 3B). Interestingly, the sequences complementary to the siRNA guide strand are localized in different parts of these genes: in the 5′ UTR (SLC16A2), in exons (MINK1), or the last exon/3′ UTR (PEG3), depending on the splice variant of the PEG3 transcript (Figure 3C). The effects of PEG3 silencing in vivo are difficult to predict because this protein is predominantly expressed in the ovary, testis, and placenta. The maternal allele of PEG3 is inactive, and only the paternal allele is functional throughout the lifetime of mammals.[39,40] Human PEG3 carries 12 zinc finger DNA-binding motifs and may play a role in transcription, cell proliferation, and p53-mediated apoptosis. Therefore, the level of PEG3 and other potential off-target transcripts expressed in the CNS should be carefully evaluated in a more relevant model in vivo.

DISCUSSION

Here, we demonstrated the efficacy and allele selectivity of CAG-targeting shRNAs in four models of polyQ diseases. These results are an important step toward the development of universal drugs for polyQ diseases with the use of RNAi tools and repeat-targeting strategy. One of the most important features/advantages of the proposed strategy, distinguishing it from the currently developed approaches, is the preferential silencing of mutant proteins. Both huntingtin and other polyQ proteins are widely expressed in the CNS and in the periphery. These proteins play important functions, such as axonal vesicular trafficking (HTT), transcription regulation (HTT, ATN-1, ATXN-7), deubiquitination (ATXN-3), and the stabilization of the cytoskeletal network (ATXN-7).[41–43] It has been demonstrated that the partial reduction of the wild-type huntingtin (∼45%) in the striatum of adult rhesus monkeys treated with AAV2-shRNA is tolerated for at least 5 months without causing motor dysfunction or marked pathology.[44] However, we still do not know the consequences of the knockdown of normal polyQ proteins in patient brains that lasts for decades.[45] Therefore, the development of therapeutic approaches based on the selective inhibition of only mutant protein with leaving the wild-type intact for normal cellular function would

be a desirable option for clinical studies. It has been proved recently that such an idea is feasible. Zinc finger proteins (ZFPs) linked to the Krüppel-associated box (KRAB) transcriptional repression domain were used to directly bind mutant CAG repeats in the HTT gene and repress transcription in an allele-selective way.[20] Although repression was highly dependent on the length of the polyCAG tract, these ZFPs selectively repressed 100% of fully-penetrant mutant HTT alleles and preserved the normal HTT expression in more than 86% of patients.

Contrary to the principles of designing functional siRNAs,[46] our shRNAs consist of repetitive, GC-rich sequences that do not contain an A or U at the 5′ end of the siRNA guide strand or AU richness at the 5′ one-third region of the siRNA guide strand.[47] Nonetheless, all shRNAs are efficiently processed by Dicer, resulting in desired strand bias and siRNA guide strands mostly with an A or G substitution at position 8 from the 5′ end. Both siRNA and miRNA identify and bind to their targets primarily through the seed region (2–7 nt), wherein base-pairing at nucleotide 8 can subsequently stabilize the duplex. The use of synthetic siRNA oligonucleotides has shown that the mismatch type and its position are crucial for the preferential silencing of the mutant proteins in the CAG-repeat targeting strategy.[27,30,31] In our study, we demonstrated that allele selectivity depends mainly on the target (polyQ model) and shRNA concentration and less on the mismatch type (A versus G). However, in case of the HD model, we observed a significant difference between the selectivity of shA2R and shG2, which differ only in mismatch type. shA2R and shA2R1 induced strong allele selectivity in fibroblasts whereas shG2 silenced both alleles. Interestingly, shG2 was the most potent and selective reagent in the luciferase tests with the IC_{50} of 10 ng for the 85CAG_Luc reporter. It may be explained by the small RNA NGS data showing that the number of reads from the G2 siRNA guide strand significantly outperforms those for other reagents (Figure S2).

The stability of the duplex formed between the guide siRNA strand and the target transcript is important for the miRNA-like translation inhibition mechanism. Therefore, we concluded that mismatched nucleotide at position 8 is important to ensure unstable interactions with normal tract and otherwise more stable interactions of multiple siRISC with expanded CAG repeats, which results in preferential silencing of mutant alleles. By comparing the allele selectivity of shRNAs in four polyQ models with similar lengths of the repeat tract, we demonstrated that other factors, such as localization of the CAG repeats within transcripts, flanking sequence composition, or target transcript to shRNA ratio, may further influence and modulate the efficacy and selectivity of silencing.

The shRNAs, which mimic natural pre-miRNAs, belong to the first generation of genetic RNAi triggers. Delivered to cells as viral vectors, these molecules allow for longer-lasting silencing effects compared to synthetic siRNAs or ASOs. There are a number of studies describing the successful use of shRNAs in the non-allele-selective silencing of polyQ genes.[44,48–50] Designing shRNA in an allele-selective

strategy utilizing SNP or the difference in CAG tract length is more demanding. The activity of SNP-targeting shRNAs was demonstrated in cellular and animal models of HD,[51] SCA3,[52,53] and SCA7,[54] whereas CAG-targeting genetic vectors have not been extensively studied to date.[30,36,37]

The high level of shRNA expression was shown to overload the endogenous miRNA biogenesis pathway[42] and induced strong toxicity *in vivo*.[55–57] Interestingly, not all shRNA vectors expressed under the strong U6 promoter were able to induce neurotoxicity in a mouse model of HD.[55] The toxic shRNAs generated higher levels of antisense siRNA strands compared with nontoxic shRNA. In this study, we used a weaker RNA Pol III promoter (H1), and the number of reads in NGS study corresponding to the A2R siRNA guide strand was similar to the highly abundant miRNAs, e.g., hsa-miR-221-3p and miR-191, and about two times lower than for miR-30a (Figure S4). The problem of the saturation of the miRNA biogenesis pathway by overexpression of shRNAs may also be overcome by the use of artificial miRNAs, the second generation of siRNA expressing vectors, which mimic the pri-miRNAs.[55,58] However, the poorly controlled two-step processing of these molecules in cells further complicates the design of efficient and allele-selective molecules. In addition, direct comparison of shRNA- and artificial miRNA-based strategies revealed that shRNAs are more potent than the artificial miRNAs in mediating gene silencing *in vitro* and *in vivo*.[58]

The idea of one drug toward all polyQ diseases is very attractive for the pharma industry and patients suffering from these rare diseases. As we demonstrated, each polyQ model exhibited a slightly different pattern of silencing after treatment with the same shRNAs; however, shA2R selectively silenced mutant proteins in all tested models. This molecule does not produce passenger strand, which might induce off-target effects, is selective toward target genes, and does not induce significant degradation of other complementary transcripts in human fibroblast. In summary, our study supports the idea of employing CAG- targeting strategy for the treatment of polyQ diseases. We demonstrated that preferential repression of mutant proteins by vector-based RNAi tools is feasible; however, further studies performed in more relevant cellular and animal models are necessary to get this strategy on road to clinics.

MATERIALS AND METHODS

Cell Culture

Fibroblasts from HD patients (GM04208, 21/44 CAG; GM04281, 17/ 68 CAG; GM09197, 21/151 CAG in the *HTT* gene), SCA3 patient (GM06153, 18/69 CAG in the *ATXN3* gene), SCA7 (GM03561, 8/ 62 CAG in the *ATXN7* gene), and DRPLA patient (GM13717, 16/ 68 in the *ATN1* gene) were obtained from the Coriell Cell Repositories (Camden, NJ, USA) and grown in minimal essential medium (Sigma-Aldrich, St. Louis, MO, USA) supplemented with 10% fetal bovine serum (FBS) (Sigma-Aldrich) and antibiotics (Sigma-Aldrich). HEK 293T cells were grown in Dulbecco's modified Eagle's medium (Sigma-Aldrich) supplemented with 8% (FBS) (Sigma-Aldrich), antibiotics (Sigma-Aldrich) and L-glutamine (Sigma-Aldrich). Mouse

striatal cell lines (STHdh), were purchased from the Coriell Cell Repositories and grown in a medium containing DMEM (GIBCO), FBS (Sigma-Aldrich), G418, and penicillin/streptomycin, with incubator conditions of 5% CO_2 and 33°C. All cell lines used in this study are listed in the Table S2.

Plasmids and Viral Vectors

The shRNA expression cassettes were generated from DNA oligonucleotides (Sigma-Aldrich, see sequences in Table S3). shRNAs, under an H1 polymerase III promoter, comprised a 22-bp stem and 10-nt miR-23 loop. We used shScr (scrambled) or shLuc, which targets the luciferase gene, as negative controls of silencing. Pairs of oligonucleotides were annealed and ligated into the pGreenPuro (System Biosciences, Palo Alto, CA, USA) expression plasmid and verified through sequencing. For lentivirus production, the plasmids were cotransfected with the packaging plasmids pPACKH1-GAG, pPACKH1-REV, and pVSVG (System Biosciences) in HEK 293TN cells. The medium was collected at days 2 and 3, and the viral supernatants were passed through 0.45-µm filters and concentrated using PEGit Virus Precipitation Solution (System Biosciences). The lentiviral vectors were resuspended in Opti-MEM (GIBCO), and the virus titers (TU/mL) were determined through flow cytometry (Accuri C6, BD Biosciences) based on copGFP expression. The transduction of fibroblasts was performed at a MOI of 1 and/or 10 in the presence of polybrene (4 µg/mL). Total RNA and protein were harvested at 7 days posttransduction.

Luciferase Assays

For luciferase assays, HEK 293T cells were seeded in a 24-well plate at a density of 10^5 cells per well, in DMEM 1 day prior to transfection. Cells were cotransfected with shRNA expression constructs and luciferase reporters that contain both the firefly luciferase (FL) and Renilla luciferase (RL) genes (pmirGLO plasmid, Promega). Transfection was performed with Lipofectamine 2000 (Invitrogen, Thermo Fisher Scientific) according to the manufacturer's protocol. Exon 1 of the *HTT* gene with 85 or 16 CAG was fused upstream the FL gene. 48 h post-transfection, cells were harvested using Passive Lysis Buffer 1× (Promega) according to the manufacturer's instruction. Measurements of RL and FL activity were performed using Dual-Luciferase Reporter Assay (Promega). FL was normalized to RL expression. A scrambled construct (shScr) served as a negative control and was set at 1. The value of IC_{50} was calculated as a concentration of shRNA needed to reach half-maximum silencing of mutant and/or normal allele. Allele selectivity ratio for each shRNA was calculated by dividing the IC_{50} of the 16CAG_Luc reporter against the IC_{50} of the 85CAG_Luc reporter.

Western Blotting

The western blot analysis for HTT protein was performed as previously described.[30] Briefly, 25 µg of total protein was run on a Tris-acetate sodium dodecyl sulfate (SDS)-polyacrylamide gel (1.5 cm, 4% stacking gel/4.5 cm, 5% resolving gel, acrylamide:bis-acrylamide ratio of 49:1) in XT Tricine buffer (Bio-Rad, Hercules, CA, USA) at 135 V in an ice-water bath. After electrophoresis, the proteins were wet-transferred overnight to a nitrocellulose membrane (Sigma-Aldrich).

The primary and secondary antibodies were used in a PBS/0.1% Tween-20 buffer containing 5% nonfat milk. The immunoreaction was detected using Western Bright Quantum HRP Substrate (Advansta, Menlo Park, CA, USA). The protein bands were scanned directly from the membrane using a camera and quantified using Gel-Pro Analyzer (Media Cybernetics). Plectin was used as a reference protein.

For 25 μg of total protein SCA3, SCA7, and DRPLA electrophoresis, we used NuPAGE Tris-Acetate 3%–8% Protein Gels (Thermo Fisher Scientific) in NuPAGE Tris-Acetate SDS Running Buffer (Thermo Fisher Scientific). Next the proteins were wet-transferred to a nitrocellulose membrane (Sigma-Aldrich). The primary and secondary antibodies were used in a TBS/0.1% Tween-20 buffer containing 5% nonfat milk. The immunoreaction was detected as described below. Vinculin and GAPDH were used as reference proteins.

The resolution of 25 μg of total protein containing TBP (40 kDa), FOXP2 (80 kDa), RPL14 (25 kDa), MINK1 (150 kDa), PEG3 (179 kDa), SLC16A2 (60 kDa), and reference-GAPDH (40 kDa) proteins for simultaneous analysis on a single gel was performed on polyacrylamide gels (1.5 cm, 5% stacking gel/4.5 cm, 12% resolving gel, acrylamide:bis-acrylamide ratio of 29:1) in XT Tricine buffer (Bio-Rad, Hercules, CA, USA) at 120 V at room temperature. The proteins were wet-transferred to a nitrocellulose membrane (Sigma-Aldrich). The immunodetection steps were performed as described below using PBS/0.1% Tween-20 buffer containing 5% nonfat milk. A list of all antibodies used is provided in Table S4.

RNA Isolation and Reverse-Transcription Polymerase Chain Reaction (PCR)

Total RNA was isolated from fibroblast cells using TRI Reagent (Bio-Shop, Burlington, Canada) according to the manufacturer's instructions. The RNA concentration was measured using a NanoDrop spectrophotometer. A total of 500 ng of RNA was reverse transcribed at 55°C using Superscript III (Life Technologies) and random hexamer primers (Promega, Madison, WI, USA). The quality of the reverse transcription (RT) reaction was assessed through polymerase chain reaction (PCR) amplification of the GAPDH gene. Complementary DNA (cDNA) was used for qPCR using SsoAdvanced Universal SYBR R Green Supermix (Bio-Rad, Hercules, CA, USA) with denaturation at 95°C for 30 s followed by 40 cycles of denaturation at 95°C for 15 s and annealing at 60°C for 30 s. The melt curve protocol was subsequently performed for 5 s at 65°C, followed by 5 s increments at 0.5°C from 65°C to 95°C with specific primers on the CFX Connect Real-Time PCR Detection System (Bio-Rad). Data preprocessing and normalization were performed using Bio-Rad CFX Manager software (Bio-Rad). The quantitative real-time PCR primer sequences for HTT, PEG3, MINK1, and SLC16A2 are listed in the Table S5.

Small RNA Next-Generation Sequencing and Data Analysis

Total RNA was isolated (TRI reagent) from HEK 293T cells at 24 h post transfection, and the RNA quality was analyzed with an Agilent 2100 Bioanalyzer (RNA Nano Chip, Agilent). Small RNA sequencing was performed by CeGaT (Tubingen, Germany) using an Illumina HiSeq2500, 1×50 bp. Demultiplexing of the sequencing reads was performed with Illumina bcl2fastq (2.19). Adapters were trimmed with Skewer (version 0.2.2).[59] The reads in FASTQ format were then subjected to length filtering using a custom Python script, retaining only sequences longer than 15 nucleotides. Then, the reads were filtered for quality using the fastq_quality_filter tool from the FASTX-Toolkit package (http://hannonlab.cshl.edu/fastx_toolkit/). We applied −q20 and −p9 parameters, by which only reads with 95% of bases with Phred quality score ≥ 20 were retained. With quality filtering, between 5% and 6% of reads per sample were discarded. Then, we removed data redundancy with fastx_collapse from the same package. The reads were finally mapped against sequences of our shRNA constructs using Bowtie, with no mismatches allowed. Finally, with in-house Python script, the alignments were parsed and displayed in a graphical form for manual inspection.

Northern Blotting

Total RNA (35 μg) isolated from HEK 293T cells was resolved on denaturing polyacrylamide gels (12% PAA, 19:1 acrylamide/bis, and 7.5 M urea) in 0.5× TBE. The RNA was transferred to a GeneScreen Plus hybridization membrane (PerkinElmer) using semidry electroblotting (Sigma-Aldrich). The membrane was probed with a specific 21 nt DNA probe composed of CAG repeats and labeled with [γ32P] ATP (5,000 Ci/mmol, Hartmann Analytics) using OptiKinase (USB) according to the manufacturer's instructions.[60] The hybridization was performed at 37°C overnight in a buffer containing $5 \times$ SSC, 1% SDS, and 1× Denhardt's solution. The radioactive signals were quantified through phosphorimaging (Multi Gauge v3.0, Fujifilm).

Statistical Analysis

All experiments were repeated at least three times. The statistical significance of silencing was assessed using a one-sample t test, with an arbitrary value of 1 assigned to the cells treated with control shLuc. Selected data were compared using an unpaired t test. The two-tailed p values of < 0.05 were considered significant.

SUPPLEMENTAL INFORMATION

Supplemental Information can be found online at https://doi.org/10.1016/j.omtn.2019.12.012.

AUTHOR CONTRIBUTIONS

CONFLICTS OF INTEREST

REFERENCES

1. Ross, C.A. (2002). Polyglutamine pathogenesis: emergence of unifying mechanisms for Huntington's disease and related disorders. Neuron 35, 819–822.

2. Fan, H.C., Ho, L.I., Chi, C.S., Chen, S.J., Peng, G.S., Chan, T.M., Lin, S.Z., and Harn, H.J. (2014). Polyglutamine (PolyQ) diseases: genetics to treatments. Cell Transplant. 23, 441–458.

3. Sittler, A., Muriel, M.P., Marinello, M., Brice, A., den Dunnen, W., and Alves, S. (2018). Deregulation of autophagy in postmortem brains of Machado-Joseph disease patients. Neuropathology 38, 113–124.

4. Seidel, K., Siswanto, S., Brunt, E.R., den Dunnen, W., Korf, H.W., and Rüb, U. (2012). Brain pathology of spinocerebellar ataxias. Acta Neuropathol. 124, 1–21.

5. Tabrizi, S.J., Ghosh, R., and Leavitt, B.R. (2019). Huntingtin Lowering Strategies for Disease Modification in Huntington's Disease. Neuron 101, 801–819.

6. Buijsen, R.A.M., Toonen, L.J.A., Gardiner, S.L., and van Roon-Mom, W.M.C. (2019). Genetics, Mechanisms, and Therapeutic Progress in Polyglutamine Spinocerebellar Ataxias. Neurotherapeutics 16, 263–286.

7. Wild, E.J., and Tabrizi, S.J. (2017). Therapies targeting DNA and RNA in Huntington's disease. Lancet Neurol. 16, 837–847.

8. Ashizawa, T., Öz, G., and Paulson, H.L. (2018). Spinocerebellar ataxias: prospects and challenges for therapy development. Nat. Rev. Neurol. 14, 590–605.

9. Keiser, M.S., Kordasiewicz, H.B., and McBride, J.L. (2016). Gene suppression strategies for dominantly inherited neurodegenerative diseases: lessons from Huntington's disease and spinocerebellar ataxia. Hum. Mol. Genet. 25 (R1), R53–R64.

10. Olejniczak, M., Urbanek, M.O., and Krzyzosiak, W.J. (2015). The role of the immune system in triplet repeat expansion diseases. Mediators Inflamm. 2015, 873860.

11. Dickey, A.S., and La Spada, A.R. (2018). Therapy development in Huntington disease: From current strategies to emerging opportunities. Am. J. Med. Genet. A. 176, 842–861.

12. Dickey, A.S., Pineda, V.V., Tsunemi, T., Liu, P.P., Miranda, H.C., Gilmore-Hall, S.K., Lomas, N., Sampat, K.R., Buttgereit, A., Torres, M.J., et al. (2016). PPAR-δ is repressed in Huntington's disease, is required for normal neuronal function and can be targeted therapeutically. Nat. Med. 22, 37–45.

13. Esteves, S., Duarte-Silva, S., and Maciel, P. (2017). Discovery of Therapeutic Approaches for Polyglutamine Diseases: A Summary of Recent Efforts. Med. Res. Rev. 37, 860–906.

14. Monteys, A.M., Ebanks, S.A., Keiser, M.S., and Davidson, B.L. (2017). CRISPR/Cas9 Editing of the Mutant Huntingtin Allele In Vitro and In Vivo. Mol. Ther. 25, 12–23.

15. Dabrowska, M., Juzwa, W., Krzyzosiak, W.J., and Olejniczak, M. (2018). Precise Excision of the CAG Tract from the Huntingtin Gene by Cas9 Nickases. Front. Neurosci. 12, 75.

16. Ouyang, S., Xie, Y., Xiong, Z., Yang, Y., Xian, Y., Ou, Z., Song, B., Chen, Y., Xie, Y., Li, H., and Sun, X. (2018). CRISPR/Cas9-Targeted Deletion of Polyglutamine in Spinocerebellar Ataxia Type 3-Derived Induced Pluripotent Stem Cells. Stem Cells Dev. 27, 756–770.

17. Merienne, N., Vachey, G., de Longprez, L., Meunier, C., Zimmer, V., Perriard, G., Canales, M., Mathias, A., Herrgott, L., Beltraminelli, T., et al. (2017). The Self-Inactivating KamiCas9 System for the Editing of CNS Disease Genes. Cell Rep. 20, 2980–2991.

18. Shin, J.W., Kim, K.H., Chao, M.J., Atwal, R.S., Gillis, T., MacDonald, M.E., Gusella, J.F., and Lee, J.M. (2016). Permanent inactivation of Huntington's disease mutation by personalized allele-specific CRISPR/Cas9. Hum. Mol. Genet. 25, 4566–4576.

19. Tabrizi, S.J., Leavitt, B.R., Landwehrmeyer, G.B., Wild, E.J., Saft, C., Barker, R.A., Blair, N.F., Craufurd, D., Priller, J., Rickards, H., et al.; Phase 1–2a IONIS-HTTRx Study Site Teams (2019). Targeting huntingtin expression in patients with Huntington's disease. N. Engl. J. Med. 380, 2307–2316.

20. Zeitler, B., Froelich, S., Marlen, K., Shivak, D.A., Yu, Q., Li, D., Pearl, J.R., Miller, J.C., Zhang, L., Paschon, D.E., et al. (2019). Allele-selective transcriptional repression of mutant HTT for the treatment of Huntington's disease. Nat. Med. 25, 1131–1142.

21. Alterman, J.F., Godinho, B.M.D.C., Hassler, M.R., Ferguson, C.M., Echeverria, D., Sapp, E., Haraszti, R.A., Coles, A.H., Conroy, F., Miller, R., et al. (2019). A divalent siRNA chemical scaffold for potent and sustained modulation of gene expression throughout the central nervous system. Nat. Biotechnol. 37, 884–894.

22. Hersch, S., Claassen, D., Edmondson, M., Wild, E., Guerciolini, R., and Panzara, M. (2017). Multicenter, Randomized, Double-blind, Placebo-controlled Phase 1b/2a Studies of WVE-120101 and WVE-120102 in Patients with Huntington's Disease (P2.006). Neurology 2017, 88.

23. Southwell, A.L., Skotte, N.H., Kordasiewicz, H.B., Østergaard, M.E., Watt, A.T., Carroll, J.B., Doty, C.N., Villanueva, E.B., Petoukhov, E., Vaid, K., et al. (2014). In vivo evaluation of candidate allele-specific mutant huntingtin gene silencing antisense oligonucleotides. Mol. Ther. 22, 2093–2106.

24. Miller, V.M., Xia, H., Marrs, G.L., Gouvion, C.M., Lee, G., Davidson, B.L., and Paulson, H.L. (2003). Allele-specific silencing of dominant disease genes. Proc. Natl. Acad. Sci. USA 100, 7195–7200.

25. Liu, J., Yu, D., Aiba, Y., Pendergraff, H., Swayze, E.E., Lima, W.F., Hu, J., Prakash, T.P., and Corey, D.R. (2013). ss-siRNAs allele selectively inhibit ataxin-3 expression: multiple mechanisms for an alternative gene silencing strategy. Nucleic Acids Res. 41, 9570–9583.

26. Hu, J., Liu, J., Narayanannair, K.J., Lackey, J.G., Kuchimanchi, S., Rajeev, K.G., Manoharan, M., Swayze, E.E., Lima, W.F., Prakash, T.P., et al. (2014). Allele-selective inhibition of mutant atrophin-1 expression by duplex and single-stranded RNAs. Biochemistry 53, 4510–4518.

27. Hu, J., Liu, J., and Corey, D.R. (2010). Allele-selective inhibition of huntingtin expression by switching to an miRNA-like RNAi mechanism. Chem. Biol. 17, 1183–1188.

28. Hu, J., Liu, J., Yu, D., Aiba, Y., Lee, S., Pendergraff, H., Boubaker, J., Artates, J.W., Lagier-Tourenne, C., Lima, W.F., et al. (2014). Exploring the effect of sequence length and composition on allele-selective inhibition of human huntingtin expression by single-stranded silencing RNAs. Nucleic Acid Ther. 24, 199–209.

29. Hu, J., Matsui, M., Gagnon, K.T., Schwartz, J.C., Gabillet, S., Arar, K., Wu, J., Bezprozvanny, I., and Corey, D.R. (2009). Allele-specific silencing of mutant huntingtin and ataxin-3 genes by targeting expanded CAG repeats in mRNAs. Nat. Biotechnol. 27, 478–484.

30. Fiszer, A., Olejniczak, M., Galka-Marciniak, P., Mykowska, A., and Krzyzosiak, W.J. (2013). Self-duplexing CUG repeats selectively inhibit mutant huntingtin expression. Nucleic Acids Res. 41, 10426–10437.

31. Hu, J., Liu, J., Yu, D., Chu, Y., and Corey, D.R. (2012). Mechanism of allele-selective inhibition of huntingtin expression by duplex RNAs that target CAG repeats: function through the RNAi pathway. Nucleic Acids Res. 40, 11270–11280.

32. Fiszer, A., Wroblewska, J.P., Nowak, B.M., and Krzyzosiak, W.J. (2016). Mutant CAG repeats effectively targeted by RNA interference in SCA7 cells. Genes (Basel) 7, E132.

33. Fiszer, A., Ellison-Klimontowicz, M.E., and Krzyzosiak, W.J. (2016). Silencing of genes responsible for polyQ diseases using chemically modified single-stranded siRNAs. Acta Biochim. Pol. 63, 759–764.

34. Fiszer, A., Olejniczak, M., Switonski, P.M., Wroblewska, J.P., Wisniewska-Kruk, J., Mykowska, A., and Krzyzosiak, W.J. (2012). An evaluation of oligonucleotide-based therapeutic strategies for polyQ diseases. BMC Mol. Biol. 13, 6.

35. Galka-Marciniak, P., Olejniczak, M., Starega-Roslan, J., Szczesniak, M.W., Makalowska, I., and Krzyzosiak, W.J. (2016). siRNA release from pri-miRNA scaffolds is controlled by the sequence and structure of RNA. Biochim. Biophys. Acta 1859, 639–649.

36. Monteys, A.M., Wilson, M.J., Boudreau, R.L., Spengler, R.M., and Davidson, B.L. (2015). Artificial miRNAs targeting mutant huntingtin show preferential silencing in vitro and in vivo. Mol. Ther. Nucleic Acids 4, e234.

37. Miniarikova, J., Zanella, I., Huseinovic, A., van der Zon, T., Hanemaaijer, E., Martier, R., Koornneef, A., Southwell, A.L., Hayden, M.R., van Deventer, S.J., et al. (2016). Design, Characterization, and Lead Selection of Therapeutic miRNAs Targeting Huntingtin for Development of Gene Therapy for Huntington's Disease. Mol. Ther. Nucleic Acids 5, e297.

38. Kozlowski, P., de Mezer, M., and Krzyzosiak, W.J. (2010). Trinucleotide repeats in human genome and exome. Nucleic Acids Res. 38, 4027–4039.

39. Hiby, S.E., Lough, M., Keverne, E.B., Surani, M.A., Loke, Y.W., and King, A. (2001). Paternal monoallelic expression of PEG3 in the human placenta. Hum. Mol. Genet. 10, 1093–1100.

40. Jiang, X., Yu, Y., Yang, H.W., Agar, N.Y., Frado, L., and Johnson, M.D. (2010). The imprinted gene PEG3 inhibits Wnt signaling and regulates glioma growth. J. Biol. Chem. 285, 8472–8480.

41. Paulson, H.L., Shakkottai, V.G., Clark, H.B., and Orr, H.T. (2017). Polyglutamine spinocerebellar ataxias - from genes to potential treatments. Nat. Rev. Neurosci. 18, 613–626.

42. Saudou, F., and Humbert, S. (2016). The Biology of Huntingtin. Neuron 89, 910–926.

43. Wood, J.D., Nucifora, F.C., Jr., Duan, K., Zhang, C., Wang, J., Kim, Y., Schilling, G., Sacchi, N., Liu, J.M., and Ross, C.A. (2000). Atrophin-1, the dentato-rubral and pallido-luysian atrophy gene product, interacts with ETO/MTG8 in the nuclear matrix and represses transcription. J. Cell Biol. 150, 939–948.

44. Grondin, R., Kaytor, M.D., Ai, Y., Nelson, P.T., Thakker, D.R., Heisel, J., Weatherspoon, M.R., Blum, J.L., Burright, E.N., Zhang, Z., and Kaemmerer, W.F. (2012). Six-month partial suppression of Huntingtin is well tolerated in the adult rhesus striatum. Brain 135, 1197–1209.

45. Kaemmerer, W.F., and Grondin, R.C. (2019). The effects of huntingtin-lowering: what do we know so far? Degener. Neurol. Neuromuscul. Dis. 9, 3–17.

46. Naito, Y., and Ui-Tei, K. (2012). SiRNA design software for a target gene-specific RNA interference. Front. Genet. 3, 102.

47. Kamola, P.J., Nakano, Y., Takahashi, T., Wilson, P.A., and Ui-Tei, K. (2015). The siRNA Non-seed Region and Its Target Sequences Are Auxiliary Determinants of Off-Target Effects. PLoS Comput. Biol. 11, e1004656.

48. Harper, S.Q., Staber, P.D., He, X., Eliason, S.L., Martins, I.H., Mao, Q., Yang, L., Kotin, R.M., Paulson, H.L., and Davidson, B.L. (2005). RNA interference improves motor and neuropathological abnormalities in a Huntington's disease mouse model. Proc. Natl. Acad. Sci. USA 102, 5820–5825.

49. Rodriguez-Lebron, E., Denovan-Wright, E.M., Nash, K., Lewin, A.S., and Mandel, R.J. (2005). Intrastriatal rAAV-mediated delivery of anti-huntingtin shRNAs induces partial reversal of disease progression in R6/1 Huntington's disease transgenic mice. Mol. Ther. 12, 618–633.

50. Drouet, V., Perrin, V., Hassig, R., Dufour, N., Auregan, G., Alves, S., Bonvento, G., Brouillet, E., Luthi-Carter, R., Hantraye, P., and Déglon, N. (2009). Sustained effects of nonallele-specific Huntingtin silencing. Ann. Neurol. 65, 276–285.

51. Drouet, V., Ruiz, M., Zala, D., Feyeux, M., Auregan, G., Cambon, K., Troquier, L., Carpentier, J., Aubert, S., Merienne, N., et al. (2014). Allele-specific silencing of mutant huntingtin in rodent brain and human stem cells. PLoS ONE 9, e99341.

52. Nóbrega, C., Nascimento-Ferreira, I., Onofre, I., Albuquerque, D., Hirai, H., Déglon, N., and de Almeida, L.P. (2013). Silencing mutant ataxin-3 rescues motor deficits and neuropathology in Machado-Joseph disease transgenic mice. PLoS ONE 8, e52396.

53. Alves, S., Nascimento-Ferreira, I., Auregan, G., Hassig, R., Dufour, N., Brouillet, E., Pedroso de Lima, M.C., Hantraye, P., Pereira de Almeida, L., and Déglon, N. (2008). Allele-specific RNA silencing of mutant ataxin-3 mediates neuroprotection in a rat model of Machado-Joseph disease. PLoS ONE 3, e3341.

54. Scholefield, J., Watson, L., Smith, D., Greenberg, J., and Wood, M.J.A. (2014). Allele-specific silencing of mutant Ataxin-7 in SCA7 patient-derived fibroblasts. Eur. J. Hum. Genet. 22, 1369–1375.

55. McBride, J.L., Boudreau, R.L., Harper, S.Q., Staber, P.D., Monteys, A.M., Martins, I., Gilmore, B.L., Burstein, H., Peluso, R.W., Polisky, B., et al. (2008). Artificial miRNAs mitigate shRNA-mediated toxicity in the brain: implications for the therapeutic development of RNAi. Proc. Natl. Acad. Sci. USA 105, 5868–5873.

56. Grimm, D., Streetz, K.L., Jopling, C.L., Storm, T.A., Pandey, K., Davis, C.R., Marion, P., Salazar, F., and Kay, M.A. (2006). Fatality in mice due to oversaturation of cellular microRNA/short hairpin RNA pathways. Nature 441, 537–541.

57. Martin, J.N., Wolken, N., Brown, T., Dauer, W.T., Ehrlich, M.E., and Gonzalez-Alegre, P. (2011). Lethal toxicity caused by expression of shRNA in the mouse striatum: implications for therapeutic design. Gene Ther. 18, 666–673.

58. Boudreau, R.L., Monteys, A.M., and Davidson, B.L. (2008). Minimizing variables among hairpin-based RNAi vectors reveals the potency of shRNAs. RNA 14, 1834–1844.

59. Jiang, H., Lei, R., Ding, S.W., and Zhu, S. (2014). Skewer: a fast and accurate adapter trimmer for next-generation sequencing paired-end reads. BMC Bioinformatics 15, 182.

60. Koscianska, E., Starega-Roslan, J., Sznajder, L.J., Olejniczak, M., Galka-Marciniak, P., and Krzyzosiak, W.J. (2011). Northern blotting analysis of microRNAs, their precursors and RNA interference triggers. BMC Mol. Biol. 12, 14.